pH-Dependent Monomer ↔ Oligomer Interconversion of Copper(II) Complexes with *N*-(2-R-imidazol-4-ylmethylidene)-2-aminoethylpyridine (R = Methyl, Phenyl)

Naohide Matsumoto,*,† Yuri Motoda,† Toshihiro Matsuo,† Toshio Nakashima,‡ Nazzareno Re,§ Francoise Dahan,|| and Jean-Pierre Tuchagues*,||

Department of Chemistry, Faculty of Science, Kumamoto University, Kurokami 2-39-1, Kumamoto 860-8555, Japan, Faculty of Education, Oita University, Dan-noharu 700, Oita 870-1192, Japan, Dipartmento di Chimica, Universita di Perugia, via Elce di Sotto 8, 06100 Perugia, Italy, and Laboratoire de Chimie de Coordination du CNRS, UP 8241, 205 Route de Narbonne, 31077 Toulouse Cedex, France

Received September 28, 1998

The monomer ↔ oligomer interconversion of the reported metal complexes is generated by proton abstraction/supply as a common external information input. The mononuclear copper(II) complexes **1** and **2** with [$CuCl_2$-(HL^n)] chemical formula have been prepared (HL^1 = *N*-(2-methylimidazol-4-ylmethylidene)-2-aminoethylpyridine; HL^2 = *N*-(2-phenylimidazol-4-ylmethylidene)-2-aminoethylpyridine). The crystal structures were determined. **1**·H_2O, $C_{12}H_{16}N_4OCl_2Cu$: $a = 13.773(2)$ Å, $b = 8.245(2)$ Å, $c = 13.861(2)$ Å, $\beta = 110.10(1)°$, monoclinic, $P2_1/n$, and $Z = 4$. **2**, $C_{17}H_{16}N_4Cl_2Cu$: $a = 7.6659(7)$ Å, $b = 16.287(1)$ Å, $c = 14.103(1)$ Å, $\beta = 95.058(7)°$, monoclinic, $P2_1/c$, and $Z = 4$. Complexes **1**·H_2O and **2** assume a pentacoordinated square pyramidal geometry with a N_3Cl_2 donor set consisting of the nitrogen atoms of the protonated tridentate ligand and two chloride ions in the solid state, while in aqueous solution the Cu(II) ion is tetracoordinated (N_3Ow donor set). When **1** and **2** are treated with an equimolar amount of sodium hydroxide or triethylamine, the deprotonation of the imidazole moiety promotes a self-assembly process, arising from coordination of the imidazolate nitrogen atom to a Cu(II) ion of an adjacent unit, to yield compounds **1′**·$4H_2O$ as the perchlorate salt, and **2′a**·$6H_2O$ as the perchlorate salt and **2′b** as the hexafluorophosphate salt, respectively. **1′**·$4H_2O$, $C_{12}H_{15}N_4O_5ClCu$: $a = b = 13.966(2)$ Å, $c = 33.689(3)$ Å, tetragonal, $I4_1/a$, and $Z = 16$. **2′a**·$6H_2O$, $C_{51}H_{51}N_{12}O_{15}Cl_3Cu_3$: $a = 15.177(3)$ Å, $b = 15.747(3)$ Å, $c = 14.128(3)$ Å, $\alpha = 100.06(2)°$, $\beta = 110.37(2)°$, $\gamma = 63.54(1)°$, triclinic, $P\bar{1}$, and $Z = 2$. **2′b**, $C_{17}H_{15}N_9F_6PCu$: $a = b = 29.812(5)$ Å, $c = 11.484(3)$ Å, trigonal, $R\bar{3}$, and $Z = 18$. The nuclearity of the self-assembled molecules and their detailed structure were confirmed to be cyclic imidazolate-bridged tetranuclear for **1′**·$4H_2O$ and hexanuclear for **2′a**·$6H_2O$ and **2′b**, respectively, through single-crystal X-ray analyses and FAB-MS spectra. Variable-temperature experimental magnetic susceptibility data were well reproduced by using the Heisenberg model based on a cyclic tetranuclear structure for **1′** and a cyclic hexanuclear structure for **2′a** and **2′b**. The reversible interconversion between the protonated monomeric and deprotonated oligomeric species were confirmed by pH-dependent potentiometric and electronic spectral titrations in aqueous solution, whereas the Pd(II) complex did not show a perfect disassembly process.

Introduction

Self-assembly processes involving metal ions have attracted much attentions in the field of supramolecular chemistry[1] and crystal engineering[2] from the viewpoints of the development of novel functional materials. The essential feature of self-assembly is the use of modular building blocks which contains sufficient structural information to guide the self-assembly reaction. A metal ion together with ligands contain a variety of structural information to guide the self-assembly reaction, and a number of interesting self-assembled systems have been reported in the past decade.[3] One recent interest in the field of supramolecular chemistry is to design and synthesize supramolecules exhibiting switching ability, i.e. their structure and/or physical and chemical properties change owing to the input of some external information. Electrochemical interconversion

* To whom correspondence should be addressed. Fax: +81-96-342-3390. E-mail: naohide@aster.sci.kumamoto-u.ac.jp.

† Kumamoto University.

‡ Oita University.

§ Universita di Perugia.

|| Laboratoire de Chimie de Coordination du CNRS, Toulouse.

(1) (a) Lehn, J.-M. *Supramolecular Chemistry*; VCH: Weinheim, 1995. (b) Lehn, J.-M. *Angew. Chem., Int. Ed. Engl.* **1990**, *29*, 1304. (c) *Transition Metals in Supramolecular Chemistry*; Fabbrizzi, L., Poggi, A., Eds.; ASI Kluwer Academic Publishers: Dordrecht, 1994. (d) Vogtle, F. *Supramolecular Chemistry*; Wiley: 1991. (e) Ashton, P. R.; Philip, D.; Spencer, N.; Stoddart, J. F. *J. Chem. Soc., Chem. Commun.* **1992**, 1124.

(2) (a) Desiraju, G. R. *Crystal Engineering, The Design of Organic Solids*; Elsevier: Amsterdam, 1989. (b) Kahn, O. *Molecular Magnetism*; VCH: Weinheim, 1993. (c) Abrahams, B. F.; Hoskins, B. F.; Michail, D. M.; Robson, R. *Nature* **1994**, *369*, 727. (d) Kawata, S.; Kitagawa, S.; Kumagai, H.; Kudo, C.; Kamesaki, H.; Ishiyama, T.; Suzuki, R.; Kondo, M.; Katada, M. *Inorg. Chem.* **1996**, *35*, 4449. (e) Yaghi, O. M.; Li, G.; Li, H. *Nature* **1995**, *378*, 703. (f) Miyasaka, H.; Matsumoto, N.; Okawa, H.; Re, N.; Gallo, E.; Floriani, C. *J. Am. Chem. Soc.* **1996**, *118*, 981.

(3) (a) Lehn, J.-M. *J. Coord. Chem.* **1992**, *27*, 3. (b) Baxter, P.; Lehn, J.-M.; Cian, A. D.; Fischer, J. *Angew. Chem., Int. Ed. Engl.* **1993**, *32*, 69. (c) Gelling, O. J.; Bolhuis, F.; Fering, B. L. *J. Chem. Soc., Chem. Commun.* **1991**, 917. (d) Fujita, M.; Kwon, Y. J.; Sasaki, O.; Yamaguchi, K.; Ogura, K. *J. Am. Chem. Soc.* **1995**, *117*, 7287. (d) Constable, E. C. *Nature* **1990**, *346*, 314. (f) Constable, E. C.; Ward, M. D. *J. Am. Chem. Soc.* **1990**, *112*, 1256. (g) Goodgame, D. M. L.; Williams, D. J.; Winpenny, R. E. P. *J. Chem. Soc., Dalton Trans.* **1991**, 917. (h) Goodgame, D. M. L.; Khaled, A. M.; O'Mahoney, C. A.; Williams, D. J. *J. Chem. Soc., Chem. Commun.* **1990**, 851. (i) Carina, R. F.; Bernardinelli, G.; Williams, A. F. *Angew. Chem., Int. Ed. Engl.* **1993**, *32*, 1463. (j) Ruttimann, S.; Piguet, C.; Bernardinelli, G.; Bocquet, B.; Quattropani, A.; Williams, A. F. *J. Am. Chem. Soc.* **1992**, *114*, 7440.

10.1021/ic981158b CCC: $18.00
Published on Web 03/04/1999

between a double-helical binuclear Cu(I) complex and a single-strand Cu(II) complex, electrochemical interconversion of the location of a copper ion between Cu(I) in the [12]-S_2N_2 site and Cu(II) in the [15]-N_2O_3 site of a heterotropic macrocyclic ligand, and other switching processes have been reported.[4]

As a further development of this fascinating area of supramolecular chemistry, a supramolecule reversibly interconverting between monomeric modular building blocks and self-assembled oligomers by input of external information would be of the utmost interest. The closest documented reactions which can be considered as interconversions of metal complexes between monomers and self-assembled oligomers are olation and oxolation reactions affording iso- or heteropolyanions.[5] However, these reactions do not allow control of the nuclearity and structure of the generated oligomeric species as they involve only H_2O-derived species as ligands. They generally afford several oligomeric species, the equilibrium between them being usually established very slowly (months). From this point of view, we have focused on metal complexes with a multidentate ligand containing one imidazole moiety, in which interconversion between monomers and self-assembled oligomers or polymers is achieved through proton abstraction/supply.[6] In such complexes, the monomer is stabilized as a protonated species under acidic conditions, while under basic conditions the coordinating ability of the generated imidazolate nitrogen atom stabilizes an imidazolate-bridged oligonuclear complex. Several factors control the characteristics of the self-assembly process.[7] An appropriate choice of ligand framework and/or metal ion may yield a chosen self-assembled structure, owing to the independent but additive steric restrictions imposed by the ligand framework and the preferred geometry of the metal ion upon self-assembly. It is also expected that the building and disassembling processes may result from pH-dependent formation and cleavage of metal−imidazolate nitrogen coordination bonds between adjacent units. In this contribution, we report the synthesis and molecular crystal structure of the mononuclear Cu(II) complexes **1** and **2** with *N*-(2-substituted-imidazol-4-ylmethylidene)-2-aminoethylpyridine tridentate ligands, and of the corresponding deprotonated and self-assembled tetranuclear (**1′**) and hexanuclear (**2′**) compounds, where the 2-substituent is methyl for **1**(**1′**) and phenyl for **2**(**2′**). The pH-dependent reversible interconversion between the protonated (**1**, **2**) and deprotonated (**1′**, **2′**) forms and the 2-imidazole substituent dependent nuclearity of the self-assembled **1′**and **2′** molecules (Scheme 1) are evidenced, and the magnetic properties of the oligomeric species **1′** and **2′** are interpreted.

Scheme 1. pH-Dependent Interconversions between Mononuclear (Protonated Ligand) and Self-Assembled Oligomeric (Deprotonated Ligand) Complexes: (Top) **1** ↔ **1′**; Bottom: **2** ↔ **2′**

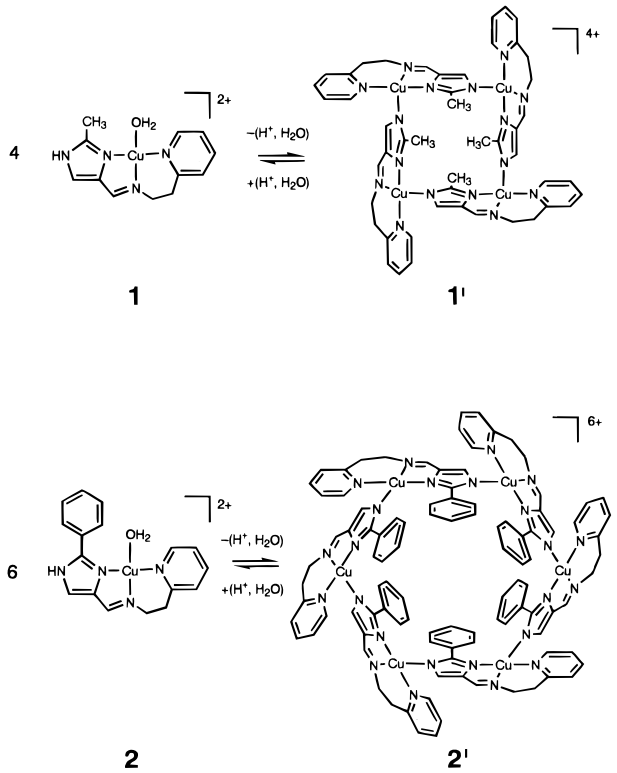

Experimental Section

Caution! *Perchlorate salts of metal complexes with organic ligands are potentially explosive. Only small amounts of materials should be prepared, and the samples should be handled with extreme caution.*

Materials. All chemicals and solvents used for the syntheses were of reagent grade and used as received. Reagents used for the physical measurements were of spectroscopic grade.

[$CuCl_2(HL^1)$] (1). A methanolic solution (20 mL) of 2-aminoethylpyridine (1.22 g, 10 mmol) was added to a methanolic solution (50 mL) of 2-methyl-4-formylimidazole (1.10 g, 10 mmol), and the mixture was stirred on a hot plate for 1 h. A methanolic solution (30 mL) of $CuCl_2 \cdot 2H_2O$ (1.70 g, 10 mmol) was then added to the HL^1 ligand solution. The reaction mixture was stirred for 10 min and filtered, and the filtrate was allowed to stand for several days. Meanwhile, vivid blue-green crystals formed which were collected by suction filtration, washed with diethyl ether, and dried in vacuo under P_2O_5. $\Lambda_M = 203$ S cm^2 mol^{-1} in water, $\Lambda_M = 69$ S cm^2 mol^{-1} in methanol. λ_{max} in water 682 nm ($\epsilon = 48$ M^{-1} cm^{-1}). IR (cm^{-1}): ν_{N-H} 3060; $\nu_{C=N}$ 1635. The single-crystal X-ray analysis described later revealed that the crystal contains one crystal water molecule, but the elemental analysis, dried well, agreed with the chemical formula without the water molecule. Anal. Calcd for $C_{12}H_{14}Cl_2CuN_4$: C, 41.33; H, 4.05; N, 16.07. Found: C, 41.41; H, 4.09; N, 16.00.

[$CuCl_2(HL^2)$] (2). Complex **2** was prepared in the form of vivid green crystals from 2-phenyl-4-formylimidazole, as described for **1**. $\Lambda_M = 200$ S cm^2 mol^{-1} in water and $\Lambda_M = 81$ S cm^2 mol^{-1} in methanol. λ_{max} in water 681 nm ($\epsilon = 59$ M^{-1} cm^{-1}). IR (cm^{-1}): ν_{N-H} 2950; $\nu_{C=N}$ 1645. Anal. Calcd for $C_{17}H_{16}Cl_2CuN_4$: C, 49.71; H, 3.93; N, 13.64. Found: C, 49.51; H, 3.93; N, 13.47.

[$Cu_4(L^1)_4$](ClO_4)$_4$ (1′). Triethylamine (1 mmol) was added to a H_2O−MeOH solution (20 mL) of **1** (0.34 g, 1 mmol), and the mixture was stirred on a hot plate for 10 min. A methanolic solution (10 mL) of $NaClO_4$ (0.12 g, 1 mmol) was then added, and the resulting reaction mixture was stirred for 10 min and filtered. The filtrate was left to stand overnight, during which time dark green-blue crystals formed.

(4) Lehn, J.-M. *Supramolecular Chemistry*; VCH: Weinheim, 1995; Section 8−5.
(5) See for example Kepert, D. L. *Comprehensive Inorganic Chemistry*; Pergamon Press: Oxford, 1973; Vol. 4, pp 607−620.
(6) (a) Matsumoto, N.; Mizuguchi, Y.; Mago, G.; Eguchi, S.; Miyasaka, H.; Nakashima, T.; Tuchagues, J.-P. *Angew. Chem., Int. Ed. Engl.* **1997**, *36*, 1860. (b) Matsumoto, N.; Nozaki, T.; Usio, H.; Motoda, K.; Ohba, M.; Mago, G.; Okawa, H. *J. Chem. Soc., Dalton Trans.* **1993**, 2157. (c) Nozaki, T.; Ushio, H.; Mago, G.; Matsumoto, N.; Okawa, H.; Yamakawa, Y.; Anno, T.; Nakashima, T. *J. Chem. Soc., Dalton Trans.* **1994**, 2339.
(7) (a) Matsumoto, N.; Yamashita, S.; Ohyoshi, A.; Kohata, S.; Okawa, H. *J. Chem. Soc., Dalton Trans.* **1988**, 1943. (b) Matsumoto, N.; Mimura, M.; Sunatsuki, Y.; Eguchi, S.; Mizuguchi, Y.; Miyasaka, H.; Nakashima, T. *Bull. Chem. Soc. Jpn.* **1997**, *70*, 2354. (c) Mimura, M.; Matsuo, T.; Nakashima, T. Matsumoto, N. *Inorg. Chem.* **1998**, *37*, 3553. (d) Mimura, M.; Matsuo, T.; Matsumoto, N.; Takamizawa, S.; Mori, W.; Re, N. *Bull. Chem. Soc. Jpn.* **1998**, 71, 1831. (e) Miyasaka, H.; Okamura, S.; Nakashima, T.; Matsumoto, N. *Inorg. Chem.* **1997**, *36*, 4329. (f) Mimura, M.; Matsuo, T.; Matsumoto, N.; Nakashima, T.; Kojima, M. *Chem. Lett.* **1998**, 691.

They were collected by suction filtration, washed with a small amount of methanol, and dried in vacuo under P_2O_5. The crude crystals were recrystallized from a mixture of water/methanol. $\Lambda_{Cu} = 99$ S cm^2 mol^{-1} in water. λ_{max} in water 620 nm ($\epsilon = 127$ M^{-1} cm^{-1}). IR (cm^{-1}): $\nu_{C=N}$ 1620; ν_{Cl-O} 1160, 1090. The single-crystal X-ray analysis described later revealed that the crystal contains four water molecules per tetranuclear complex weakly coordinated to Cu(II) ion, but the crystal easily efflorescenced and the elemental analysis agreed with the chemical formula without the water molecules. Anal. Calcd for $C_{12}H_{13}ClCuO_4N_4$: C, 38.31; H, 3.48; N, 14.89. Found: C, 38.06; H, 3.70; N, 14.46.

$[Cu_6(L^2)_6](ClO_4)_6$ (2′a). Complex **2′a** was prepared from **2** in the form of dark green prismatic crystals, as described for **1′**. $\Lambda_{Cu} = 98$ S cm^2 mol^{-1} in water. λ_{max} in water 630 nm ($\epsilon = 105$ M^{-1} cm^{-1}). IR data (cm^{-1}): $\nu_{C=N}$ 1625; ν_{Cl-O} 1180, 1090. The single-crystal X-ray analysis described later revealed that the crystal contains six crystal water molecules per hexanuclear complex, but the crystal easily efflorescenced and the elemental analysis agreed with the chemical formula without the water molecules. Anal. Calcd for $C_{17}H_{15}ClO_4CuN_4$: C, 46.58; H, 3.45; N, 12.78. Found: C, 47.20; H, 3.53; N, 12.82.

$[Cu_6(L^2)_6](PF_6)_6$ (2′b). A methanolic solution (20 mL) of $NaPF_6$ (0.3 mmol) was added to the methanolic solution of **2′a** (0.2 mmol), and the mixture was stirred and filtered. The filtrate was left to stand for several days during which time hexagonal-shaped green platelets were obtained.

Physical Measurements. Elemental C, H, and N analyses were carried out at the Elemental Analysis Service Center of Kyushu University. Infrared spectra were recorded on a JASCO IR-810 spectrophotometer using KBr disks. Electrical conductivity measurements were carried out on a Denki Kagaku Keiki AOL-10 digital conductometer in ca. 10^{-3} M solutions. Electronic spectra were recorded on a Hitachi U-4000 multipurpose recording spectrophotometer. FAB-MS spectra were recorded on a JEOL JMS-SX/SX102A tandem mass spectrometer, with a 6.0 kV source producing the positive-ion current; 3-nitrobenzyl alcohol was used as the matrix without solvent. Magnetic susceptibilities were measured with a MPMS5 SQUID susceptometer (Quantum Design Inc.) in the 2−300 K temperature range under the external magnetic field of 0.5 T. The calibrations were made with palladium. Corrections for diamagnetism were applied by using Pascal's constants.[8] Effective magnetic moments were calculated with the equation $\mu_{eff} = 2.828(\chi_A T)^{1/2}$, where χ_A is the magnetic susceptibility per mole of copper ions.

Potentiometric pH Titrations. All titrations were carried out in a thermostated bath at 25 °C and under a 99.9995% N_2 atmosphere. Extra pure grade water with resistivity higher than 18.0 MΩ was used. The automatic buret Dosimat 665 was supplied from Metrohm Ltd. (Switzerland). The GS-5015c conjugated proton electrode and the IM-40S potentiometer were supplied from TOA. Co. Ltd. (Japan). The standard electrode potential (E_0) was first determined by Gran's plot method.[9] 80 mL of 0.15 ionic strength solution containing 0.24 mmol of metal complex and sodium chloride was titrated with a solution containing 0.1 M NaOH and 0.05 M NaCl. Immediately after forward titration the resulting solution was titrated back with a solution containing 0.1 M HCl and 0.05 M NaCl. All titrations and potential measurements were PC controlled. The electrode potentials were converted into proton concentration scale ($-\log[H^+] = (E_0(\text{mV}) - E(\text{mV}))/59.15$), and the proton association degree, n, was calculated by Bjerrum's method for the forward and reverse titrations, respectively.[10]

pH Dependent Electronic Spectra. pH-Dependent electronic spectral changes were recorded at room temperature upon sequential addition of 0.1 M aqueous NaOH and HCl solutions for the forward and reverse titrations, respectively. An aqueous solution of the protonated complex (0.24 mmol of the complex in 80 mL of water) was prepared. A spectrum was recorded after each 0.4 mL addition of a 0.1 M NaOH solution, until 1 equiv of NaOH was added. Immediately after, electronic spectra were recorded for the reverse titration, following each 0.4 mL addition of a 0.1 M HCl solution to the solution resulting from the forward titration. The spectra were corrected for the volume variation due to the addition of the NaOH and HCl solutions.

X-ray Data Collection, Reduction, and Structure Determination. Complexes $1\cdot H_2O$, $1'\cdot 4H_2O$, and $2'a\cdot 6H_2O$. X-ray data were collected on a Rigaku AFC7R diffractometer with graphite monochromated Mo Kα radiation ($\lambda = 0.710\,69$ Å) and a 12 kW rotating anode generator. The single crystals of $\mathbf{1'}\cdot 4H_2O$ and $\mathbf{2'a}\cdot 6H_2O$ used for the X-ray analyses were cut from thin platelets and encapsulated in Lindemann glass capillaries containing a small amount of mother liquid. The data were collected at 20 ± 1 °C using the $\omega-2\theta$ scan technique to a maximum 2θ value of 50.0° at a scan speed of 8.0−16.0°/min (in ω). The weak reflections ($I < 10\sigma(I)$) were rescanned (maximum of 5 scans), and the counts were accumulated to ensure good counting statistics. Stationary background counts were recorded on each side of the reflection. The ratio of peak to background counting time was 2:1. The intensities of three representative reflections were measured after every 150 reflection. Over the course of the data collections, the standards reflections were monitored and decay corrections were applied through polynomial corrections. Empirical absorption corrections based on azimuthal scans of several reflections were applied. The data were also corrected for Lorentz and polarization effects.

The structures were solved by direct methods[11] and expanded using Fourier techniques.[12] $\mathbf{1}\cdot H_2O$ contains a water molecule as the crystal solvent. $\mathbf{1'}\cdot 4H_2O$ contains one perchlorate ion in the unsymmetric unit which is suffered from disorder. There are three possible positions (*a*, *b*, and *c*) for one perchlorate ion, where the population factors of 0.5, 0.25, and 0.25 were assigned for *a*, *b*, and *c*, respectively. The oxygen atoms for *b* and *c* were not determined due to the disorder and the low electron densities on the difference Fourier map. $\mathbf{2'a}\cdot 6H_2O$ contains three water molecules as the crystal solvents in the asymmetric unit, and the oxygen atoms of one of the three perchlorate ions are subjected to disorder. The oxygen atoms of the crystal waters and the disordered perchlorate ion were refined by the use of isotropic temperature factors. The other non-hydrogen atoms were refined anisotropically. Hydrogen atoms at their calculated positions were included in the structure factor calculation but were not refined. Full-matrix least-squares refinements were employed, where the R and R_w agreement factors were based on $I_o > 2\sigma(I_o)$. Plots of $\Sigma w(|F_o| - |F_c|)^2$ versus $|F_o|$, reflection order in data collection, $\sin\theta/\lambda$, and various classes of indices showed no unusual trends. Neutral atomic scattering factors were taken from Cromer and Waber.[13] Anomalous dispersion effects were included in F_c; the values $\Delta f'$ and $\Delta f''$ are those of Creagh and McAuley.[13] The values for the mass attenuation coefficients are those of Creagh and Hubbel.[13] All calculations were performed using the teXsan crystallographic software package of the Molecular Structure Corporation.[14]

Complexes 2 and 2′b. The crystals were sealed on glass fibers and mounted on an Enraf-Nonius CAD 4 diffractometer. The data were collected at 20 ± 1 °C using Mo Kα radiation with a graphite monochromator ($\lambda = 0.710\,73$ Å) to maximum 2θ value of 52° (**2**) and 44° (**2′b**). The crystals quality were monitored by scanning three standard reflections every 2 h. No significant variation were observed during the data collections. After corrections for Lorentz and polarization effects,[15] absorption corrections from ψ scans were applied.[16]

(8) Boudreaux, E. A.; Mulay, L. N. *Theory and Applications of Molecular Paramagnetism*; John Wiley and Sons: New York, 1976; pp 491−495.
(9) Gran, G. *Analyst* **1952**, 77, 661.
(10) Beck, M. T.; Nagypal, I. *Chemistry of Complex Equilibria*; Wiley: New York, 1990; p 44.
(11) SAPI91: Fan, H.-F. *Structure Analysis Programs with Intelligent Control*; Rigaku Corporation: Tokyo, Japan, 1991.
(12) DIRDIF92: Beurskens, P. T.; Admiraal, G.; Beurskens, G.; Bosman, W. P.; Garcia-Granda, S.; Gould, R. O.; Smits, J. M. M.; Smykalla, C. *The DIRDIF Program System*; Technical Report of the Crystallography Laboratory, University of Nijmegen: The Netherlands, 1992.
(13) (a) Creagh, D. C.; McAuley, W. J. *International Tables for Crystallography*; Wilson, A. J. C., ed.; Kluwer Academic Publishers: Boston, MA, 1992; Vol. C, Table 4.2.6.8. (b) Cromer, D. T.; Waber, J. T. *International Tables for X-ray Crystallography*; Kynoch Press: Birmingham, England, 1974; Vol. IV.
(14) *teXsan*: *Crystal Structure Analysis Package*; Molecular Structure Corporation: The Woodlands, TX, 1985 and 1992.
(15) Fair, C. K. *MOLEN*: *Molecular Structure Solution Procedures*; Enraf-Nonius: Delft, The Netherlands, 1990.

Table 1. Crystallographic Data for Complexes **1**·H_2O, **2**, **1′**·$4H_2O$, **2′a**·$6H_2O$, and **2′b**

complex	**1**·H_2O	**2**	**1′**·$4H_2O$	**2′a**·$6H_2O$	**2′b**
chem formula	$C_{12}H_{16}N_4OCl_2Cu$	$C_{17}H_{16}N_4Cl_2Cu$	$C_{12}H_{15}N_4O_5ClCu$	$C_{51}H_{51}N_{12}O_{15}Cl_3Cu_3$	$C_{17}H_{15}N_9F_6PCu$
fw	356.72	410.78	394.27	1369.02	483.84
space group	$P2_1/n$ (No. 14)	$P2_1/c$ (No. 14)	$I4_1/a$ (No. 88)	$P\bar{1}$ (No. 2)	$R\bar{3}$ (No. 148)
a, Å	13.773(2)	7.6659(7)	13.966(2)	15.177(3)	29.812(5)
b, Å	8.245(2)	16.287(1)	13.966(2)	15.747(3)	29.812(5)
c, Å	13.861(2)	14.103(1)	33.689(3)	14.128(3)	11.484(3)
α, deg	90	90	90	100.06(2)	90
β, deg	110.10(1)	95.058(7)	90	110.37(2)	90
γ, deg	90	90	90	63.54(1)	120
V, Å^3	1478.2(5)	1754.0(2)	6571.3(7)	2832.9(11)	8839(3)
Z	4	4	16	2	18
ρ_{calcd}, g cm^{-3}	1.603	1.556	1.594	1.605	1.636
λ, Å	0.710 69	0.710 73	0.710 69	0.710 69	0.710 73
T, °C	20 ± 1	20 ± 1	20 ± 1	20 ± 1	20 ± 1
μ, cm^{-1}	18.34	15.55	15.21	13.35	12.59
R^a	0.029	0.022	0.076	0.057	0.036
R_w	0.033[b]	0.057[c]	0.085[b]	0.087[b]	0.082[c]

[a] $R = \Sigma||F_o| - |F_c||/\Sigma|F_o|$. [b] $R_w = [\Sigma w(|F_o| - |F_c|)^2/\Sigma w|F_o|^2]^{1/2}$. [c] $R_w = [\Sigma w(|F_o^2| - |F_c^2|)^2/\Sigma w|F_o^2|^2]^{1/2}$.

Table 2. Selected Bond Distances (Å) and Angles (deg) for $[CuCl_2(HL^1)]$ (**1**·H_2O) and $[CuCl_2(HL^2)]$ (**2**) with Their Estimated Standard Deviations in Parentheses

	$[CuCl_2(HL^1)]$ (**1**·H_2O)	$[CuCl_2(HL^2)]$ (**2**)
Cu−Cl(1)	2.293(1)	2.2679(5)
Cu−Cl(2)	2.581(1)	2.5184(6)
Cu−N2	2.001(2)	2.061(1)
Cu−N3	2.039(2)	2.029(2)
Cu−N4	2.030(2)	2.033(2)
N2−Cu−N3	80.5(1)	81.24(6)
N2−Cu−N4	172.2(1)	171.70(6)
N3−Cu−N4	91.8(1)	90.74(6)

The structures were solved by using direct methods[17] and refined by full matrix least-squares.[18] All non-hydrogen atoms were refined anisotropically. Hydrogen atoms were found on a difference Fourier synthesis and introduced in calculations with the riding model (d(C−H) = 0.97 Å (CH_2), 0.93 Å (CH), 0.86 Å (NH)) with U_{iso} = 1.1 times that of riding atom. The atomic scattering factors and anomalous dispersion terms were taken from the standard compilation.[13] Refinements on F_o^2 for all reflections. Weighted R factors R_w and goodness of fit S were based on F_o^2, conventional R factors were based on F_o ($F_o > 4\sigma(F_o)$), with F_o set to zero for negative F_o^2. The calculations were performed on a MicroVAX 3400 and a PC computer using the programs MOLEN,[15] SHELXS-86,[17] SHELX 93,[18] and ORTEP.[19]

The crystallographic data are summarized in Table 1. The complex molecules are shown in Figures 1−4 with atom numbering. Selected bond lengths and angles with their estimated standard deviations are given in Tables 2 and 3, respectively. Complete X-ray crystallographic files are available in CIF format.

Results and Discussion

Synthesis and Property of Protonated and Deprotonated Complexes. The mononuclear Cu(II) complexes **1** and **2** with the $[CuCl_2(HL^n)]$ chemical formula (n = 1, 2) were prepared by mixing equimolar amounts of copper(II) chloride dihydrate and *N*-(2-substituted-imidazol-4-ylmethylidene)-2-aminoethylpyridine (HL^n) in methanol. HL^n results from the 1:1 Schiff base condensation of 2-aminoethylpyridine with 2-methyl-4-formylimidazole (HL^1) or 2-phenyl-4-formylimidazole (HL^2) in methanol. The infrared spectra of **1** and **2** exhibit an absorption assignable to ν_{N-H} at 3060 and 2950 cm^{-1}, respectively.[20] The molar electrical conductivity of **1** and **2** are 203 and 200 S cm^2 mol^{-1} in water and 69 and 81 S cm^2 mol^{-1} in methanol, respectively, indicating that the complexes behave as 2:1 and 1:1 electrolytes in water and methanol, respectively.[21] While in the solid-state two Cl^- anions are bonded to the Cu(II) ion as confirmed by the X-ray analyses described later, this result indicates that there are no Cu−Cl bonds in aqueous solution where water molecules instead of Cl^- are coordinated to Cu(II) ion.

These mononuclear Cu(II) complexes exhibit the following building-block characteristics allowing a simple self-assembly process:[7] (1) the complex molecule has a potential donor ability

Table 3. Selected Bond Distances (Å) and Angles (deg) in the $[Cu_4(L^1)_4]^{4+}$ and $[Cu_6(L^2)_6]^{6+}$ Cyclic Complex Cations of (**1′**·$4H_2O$) and (**2′a**·$6H_2O$ and **2′b**), Respectively, with Their Estimated Standard Deviations in Parentheses

$[Cu_4(L^1)_4]$-$(ClO_4)_4$ (**1′**·$4H_2O$)		$[Cu_6(L^2)_6]$-$(ClO_4)_6$ (**2′a**·$6H_2O$)		$[Cu_6(L^2)_6]$-$(PF_6)_6$ (**2′b**)	
Cu−N2	2.002(10)	Cu1−N2	2.052(5)	Cu−N2	2.008(3)
Cu−N3	2.009(10)	Cu1−N3	1.977(5)	Cu−N3	1.960(4)
Cu−N4	2.05(1)	Cu1−N4	2.103(5)	Cu−N4	1.993(3)
		Cu1−N5	1.976(5)		
		Cu2−N6	2.011(5)		
		Cu2−N7	1.981(5)		
		Cu2−N8	2.030(5)		
		Cu2−N9	1.963(5)		
Cu−N1*	1.976(10)	Cu3−N1*	1.975(5)	Cu−N1*	1.982(3)
		Cu3−N10	2.028(5)		
		Cu3−N11	1.981(5)		
		Cu3−N12	2.024(5)		
Cu−O1	2.528(8)	Cu2−O8	2.725(6)		
		Cu3−O7	2.670(5)		
N1*−Cu−N2	94.4(4)	N2−Cu1−N5	94.7(2)	N1*−Cu−N2	100.0(1)
		N6−Cu2−N9	96.8(2)		
		N10−Cu3−N1*	101.7(2)		
N1*−Cu−N3	151.2(4)	N3−Cu1−N5	159.1(2)	N1*−Cu−N3	159.3(1)
		N7−Cu2−N9	173.1(2)		
		N1*−Cu3−N11	155.6(2)		

[a] The asterisks denote the atom position generated by the respective symmetry operation: **1′**·$4H_2O$ ($-^1/_4 + y$, $^1/_4 - x$, $^1/_4 - z$); **2′a**·$6H_2O$ ($-x$, $-y$, $1-z$); and **2′b** ($y + ^1/_3$, $-x + y + ^2/_3$, $-z + ^2/_3$).

(16) North, A. C. T.; Phillips, D. C.; Mathews, F. S. *Acta Crystallogr., Sect. A*: *Found. Crystallogr.* **1968**, *A24*, 351.
(17) Sheldrick, G. M. *SHELXS-86: Program for Crystal Structure Solution*; University of Göttingen: Göttingen, Germany, 1986.
(18) Sheldrick, G. M. *SHELX-93. Program for the Refinement of Crystal Structures from Diffraction Data*; University of Göttingen: Göttingen, Germany, 1993.
(19) Johnson, C. K.; *ORTEP*; Report ORNL-3794; Oak Ridge National Laboratory: Oak Ridge, TN, 1965.
(20) Nakamoto, K. *Infrared and Raman Spectra of Inorganic and Coordination Compounds*, 4th ed.; John Wiley & Sons: New York, 1986.
(21) Geary, W. J. *Coord. Chem. Rev.* **1971**, *7*, 81.

at the imidazolate nitrogen atom; (2) the complex molecule has a potential acceptor ability at the substitutable coordination site; (3) although the complex molecule has potentially both donor and acceptor coordination abilities, the donor ability is concealed by the imidazole proton when it is associated with the imidazole nitrogen in the lower than pK_D pH region where the complex is thus monomeric. In the higher than pK_D pH region where the proton is dissociated, the donor ability which triggers the self-assembly process is revealed; (4) in such systems, both the self-assembly and reverse disassembling processes are externally monitored provided the metal−imidazolate nitrogen bond cleavage is also pH-dependent; (5) the nature of the resulting self-assembled molecular structure depends on the constraints imposed both by the ligand framework and the preferred metal coordination geometry.

In practice, when the protonated complexes **1** and **2** were treated with an equimolar amount of triethylamine or NaOH, the condensation occurred through formation of coordination bonds between the imidazolate nitrogen atoms and Cu(II) ions, yielding the self-assembled compounds as perchlorate (**1′**, **2′a**) and hexafluorophosphate (**2′b**) salts. The ν_{N-H} vibration observed for the **1** and **2** precursors is absent in the IR spectra of the deprotonated compounds **1′** and **2′**. The electrical conductivities per copper for **1′** and **2′** are ca. 100 S cm^2 mol^{-1} in water, indicating that the tridentate L^{n}H ligand has been deprotonated and is present in its L^n mononegative form in **1′** and **2′**. The positive ion FAB-MS spectra indicate the presence of the $[Cu_4(L^1)_4(ClO_4)_3]^+$ and $[Cu_6(L^2)_6(ClO_4)_5]^+$ molecular cations arising from the loss of one ClO_4^-, and indicating that **1′** and **2′** are tetra- and hexameric, respectively.

Molecular Structures of 1·H_2O and 2. ORTEP drawings of **1·H_2O** and **2** with the atom numbering scheme are shown in Figure 1. Relevant bond distances with their estimated standard deviations in parentheses are given in Table 2. In these similar molecular structures, the Cu(II) ion assumes a pentacoordinated geometry with a N_3Cl_2 donor set consisting of three nitrogen atoms from the tridentate ligand and two chloride ions. The Cu−N bond distances are in the 2.001(2)−2.039(2) Å (**1**·H_2O) and 2.029(2)−2.061(2) Å (**2**) ranges. The Cu−Cl(1) and Cu−Cl(2) distances are 2.293(1) and 2.581(1) Å (**1**·H_2O) and 2.2679(5) and 2.5184(6) Å, respectively (**2**). The coordination geometry is better described as a square pyramid, where the equatorial coordination sites are occupied by Cl(1) and the three N donors from the tridentate ligand, and the axial site is occupied by Cl(2).

Molecular Structure of 1′·4H_2O. ORTEP drawing of the cyclic tetranuclear complex cation of **1′**·4H_2O with the atom numbering scheme for the unique atoms is shown in Figure 2. Relevant interatomic distances and angles are given in Table 3. **1′**·4H_2O assumes an imidazolate-bridged cyclic tetranuclear structure, where the side and diagonal Cu−Cu distances are 6.084(2) and 8.084(3) Å, respectively. Each Cu(II) ion is coordinated by the three nitrogen donor atoms from the tridentate ligand and the imidazolate nitrogen of the adjacent unit with the Cu−N bond distances of the 1.976(10)−2.05(1) Å range. In addition to that, the water molecule weakly coordinates to Cu(II) ion with the distance of Cu−O = 2.528(8) Å. The coordination geometry can be described as a square pyramid.

Molecular Structures of 2′a·6H_2O and 2′b. The oligomeric compound resulting from deprotonation of **2** was obtained as a perchlorate (**2′a**·6H_2O) or an hexafluorophosphate (**2′b**) salt. Although crystals of **2′a**·6H_2O and **2′b** consist of the same imidazolate-bridged cyclic hexanuclear cation $[Cu_6(L^2)_6]^{6+}$ and perchlorate or hexafluorophosphate counteranions, they belong to different space groups: triclinic $P\bar{1}$ and trigonal $R\bar{3}$, respectively. Figure 3 shows ORTEP drawings of the asymmetric trinuclear unit of **2′a**·6H_2O with the atom numbering scheme and of the cyclic hexanuclear complex cation built from two such trinuclear units. Figure 4 shows the cyclic hexanuclear

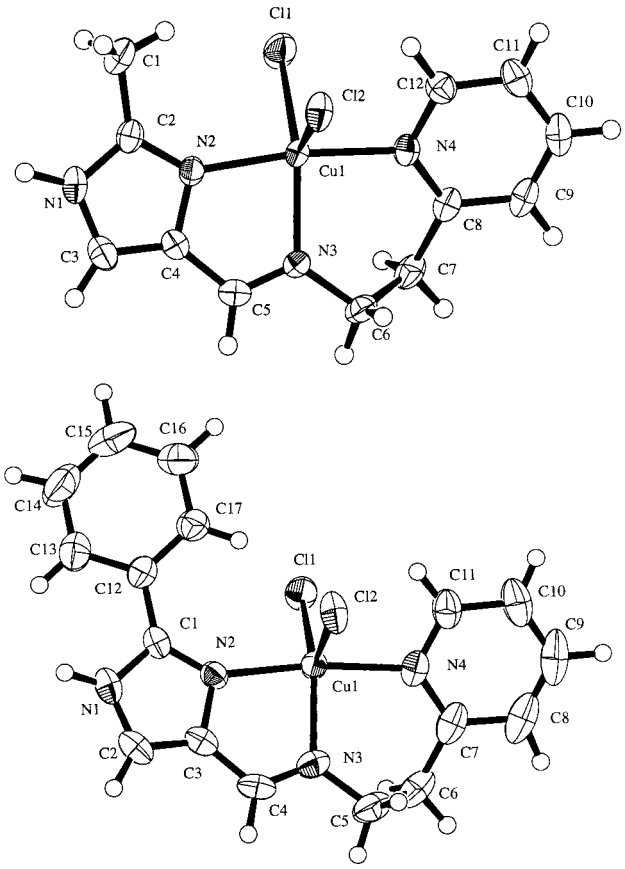

Figure 1. ORTEP drawings of [$CuCl_2HL^1$] **1**·H_2O (top) and [$CuCl_2$-(HL^2)] **2** (bottom) with the atom numbering scheme, showing 50% probability ellipsoids.

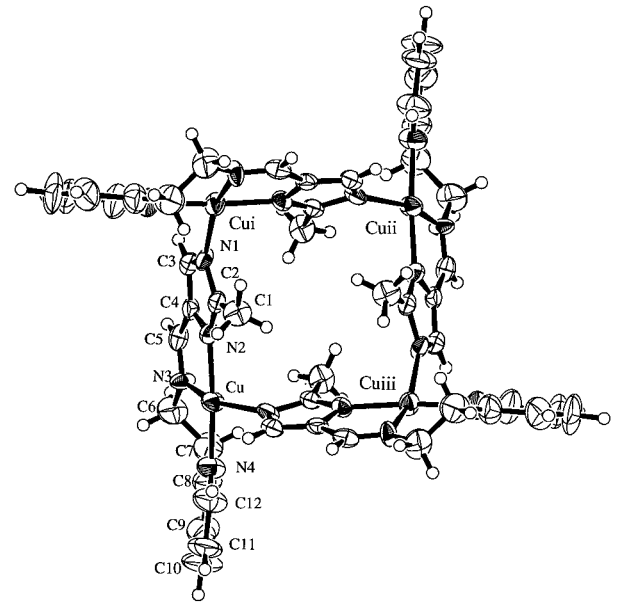

Figure 2. ORTEP drawing of the $[Cu_4(L^1)_4]^{4+}$ cyclic tetranuclear complex cation of **1′**·4H_2O with the atom numbering scheme, showing 50% probability ellipsoids. i, ii, and iii denote the positions generated by the symmetry operations of i ($^1/_4 - y$, $^1/_4 + x$, $^1/_4 - z$), ii ($-x$, $^1/_2 - y$, z), and iii ($-^1/_4 + y$, $^1/_4 - x$, $^1/_4 - z$), respectively.

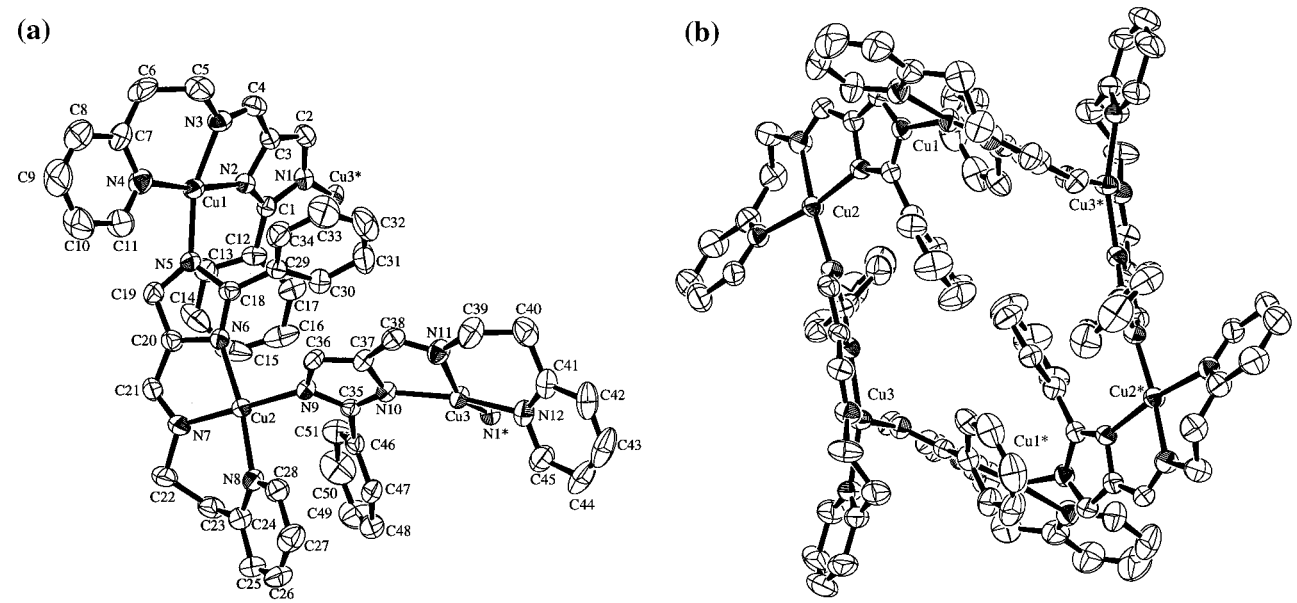

Figure 3. ORTEP drawings of (a) the asymmetric unit with the atom numbering scheme, and (b) the $[Cu_6(L^2)_6]^{6+}$ cyclic hexanuclear complex cation in **2′a**·$6H_2O$. The asterisk denotes the position generated by the symmetry operation of $(-x, -y, 1 - z)$.

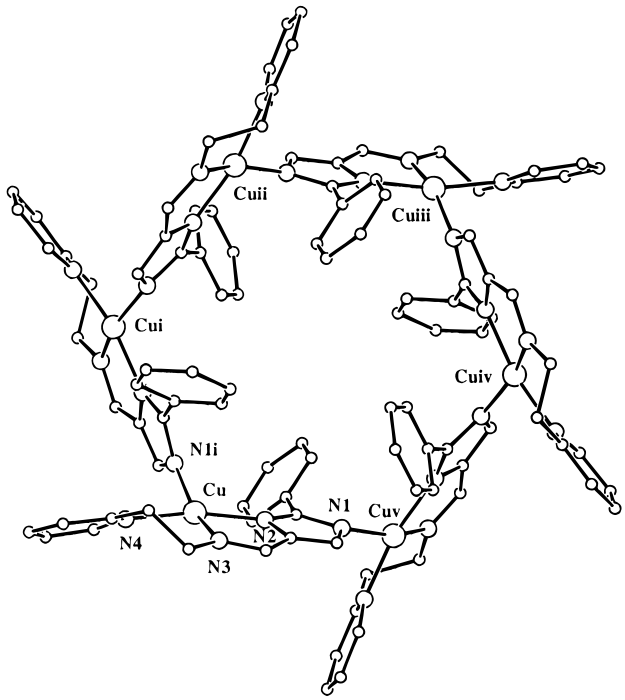

Figure 4. Molecular structure of the $[Cu_6(L^2)_6]^{6+}$ cyclic hexanuclear complex cation of **2′b**, showing the cavity. The atom numbering scheme in **2′b** is the same as in **2**. i, ii, iii, iv, and v denote the positions generated by the symmetry operations of i $(y + {}^1/_3, -x + y + {}^2/_3, -z + {}^2/_3)$, ii $(1 + y - x, 1 - x, z)$, iii $({}^4/_3 - x, {}^2/_3 - y, {}^2/_3 - z)$, iv $(1 - y, x - y, z)$, and v $(x - y + {}^1/_3, x - {}^1/_3, -z + {}^2/_3)$, respectively.

complex cation of **2′b**, in which the crystallographically unique unit consists of one Cu(II) center and one deprotonated ligand. Relevant interatomic distances and angles are summarized in Table 3. The imidazolate bridged Cu(II) centers are 6.077(2), 6.133(2), and 6.134(2) Å apart from each other in **2′a**·$6H_2O$ and 6.0273(6) Å in **2′b**. Each Cu(II) ion in **2′b** assumes a square planar coordination geometry with the three nitrogen donor atoms of the tridentate ligand and the imidazolate nitrogen of the adjacent unit with the Cu−N distances of 1.960(4)−2.008(3) Å ranges. In **2′a**·$6H_2O$, in addition to the Cu−N bonds with the distances of 1.963(5)−2.103(5) Å, there is a weak coordination bond for Cu2 and Cu3 between the oxygen atoms of perchlorate ions and copper(II) ions with the distances of Cu2−O8 = 2.725(6) Å and Cu3−O7 = 2.670(5) Å.

It is the proper stage to consider why the same self-assembly process yields cyclic tetranuclear or hexanuclear structures depending upon the nature of the 2-imidazole substituent in the otherwise identical tridentate ligands of **1** and **2**. There are no relevant differences in the four Cu−N coordination bond distances and imidazolate-bridged Cu−Cu distances between the two oligomeric structures. Among these four Cu−N bonds, the shortest involves the imidazolate nitrogen atom occupying the equatorial coordination site of the adjacent Cu(II) ion. The 2-imidazolate substituents of the adjacent modular units orient themselves in directions opposite to each other to form the imidazolate-bridged cyclic structure. Thus, the 2-imidazole substituents of the next nearest neighboring units face to each other. Therefore, concerning the strong coordination bonds resulting from the imidazolate bridges and the cyclic structure, the steric repulsion between 2-imidazolate substituents facing each other is the factor determining the orientation of adjacent modular units, and consequently the actual structure. A cyclic hexanuclear structure is more favorable than a cyclic tetranuclear structure for avoiding steric repulsion, because the Cu−Cu distance of similarly oriented modular units is increased in a cyclic hexanuclear structure. Figure 5 shows the space-filling representations of the **1′** tetranuclear and **2′** hexanuclear complex cations. The space filling drawings clearly show that the presence of bulky phenyl substituents does not allow a cyclic tetranuclear structure for steric reasons. The structural parameter determining the nuclearity is the N−Cu−N angle in the $(-Cu-Im)_n-$ macrocyclic framework. This angle is 94.4(4)° for **1′**·$4H_2O$ while it is 100.0(1)° for **2′b** and the three different N−Cu−N angles (94.7(2), 96.8(2), and 101.7(2)°) in the $P\bar{1}$ space group of **2′a**·$6H_2O$ average to 97.7°. As a whole, the N−Cu−N angle in the **1′**·$4H_2O$ cyclic tetramer is substantially smaller than in the **2′a**·$6H_2O$ and **2′b** cyclic hexamers. This angle is the key-parameter as it reflects the relative orientations of the adjacent CuL^- building units. The 2-imidazolate substituent determines the steric repulsion not only between the

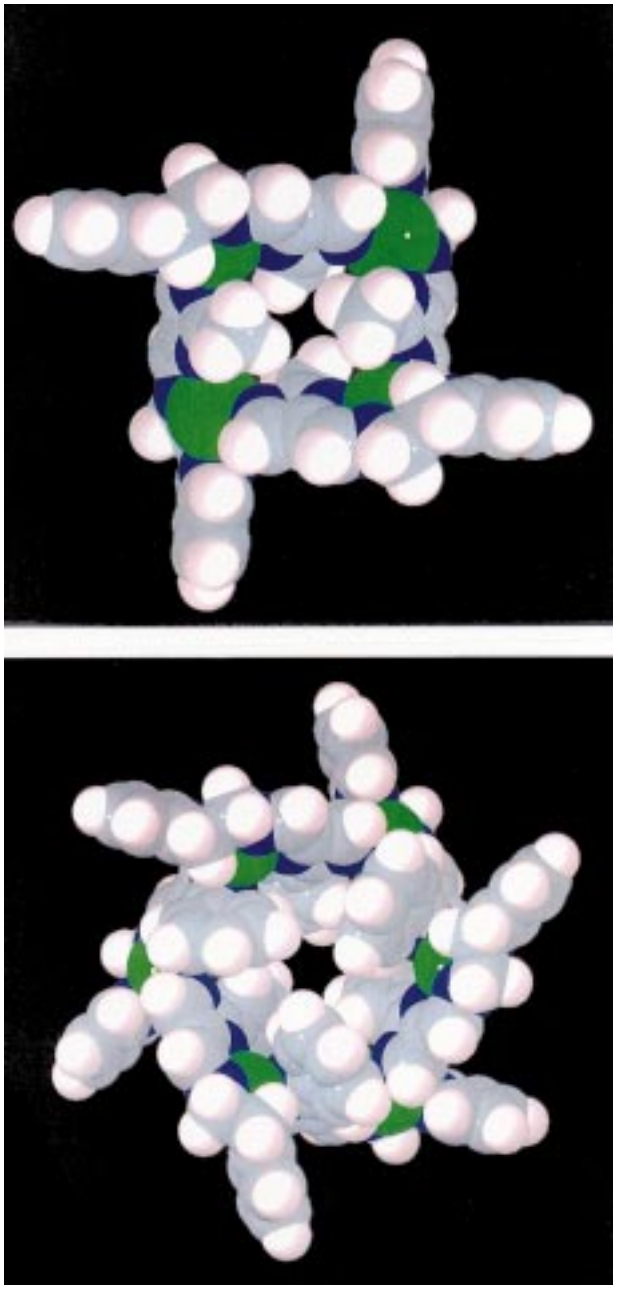

Figure 5. Space-filling representations of the cyclic complex cations of **1′** (top) and **2′b** (bottom), showing the cavity and the orientation of 2-imidazolate substituents.

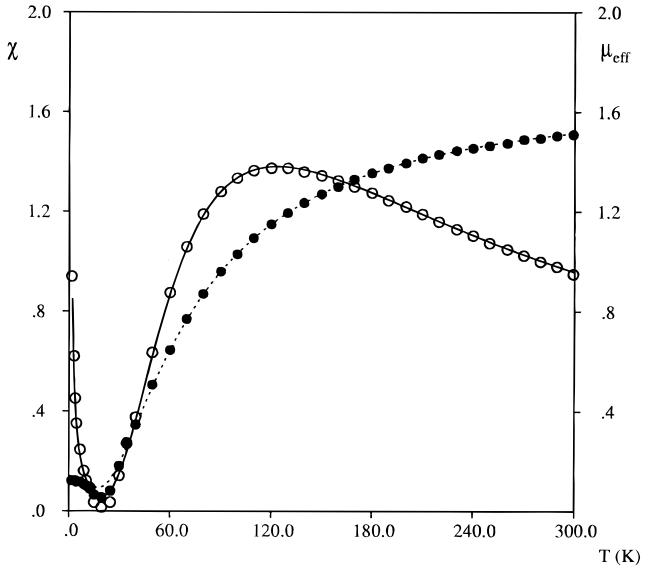

Figure 6. Plots of the magnetic susceptibility and magnetic moment per copper vs temperature for **1′**. The solid lines represent the theoretical curves obtained with the model and best-fit parameters mentioned in the text.

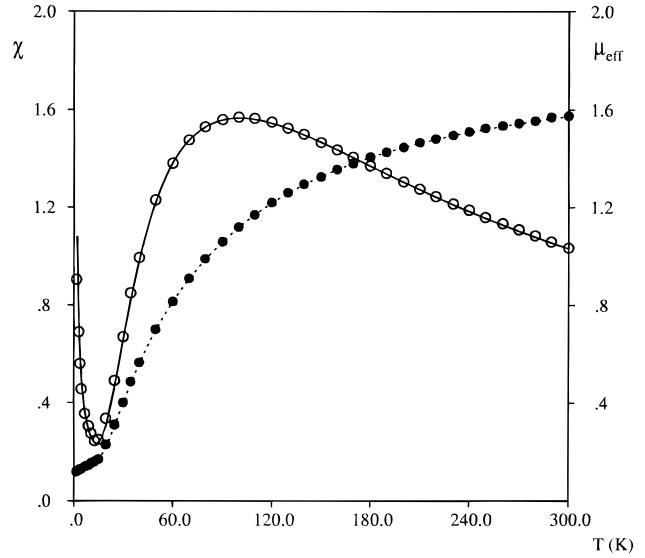

Figure 7. Plots of the magnetic susceptibility and magnetic moment per copper vs temperature for **2′b**. The solid lines represent the theoretical curves obtained with the model and best-fit parameters mentioned in the text.

adjacent CuL^- units but also between the next nearest neighboring CuL^- units upon formation of the $(-Cu-Im)_n-$ macrocyclic framework. Thus, the 2-imidazolate substituent also determines the nuclearity compatible with the flexibility of the Cu(II) coordination environment.

Magnetic Susceptibility Studies. The magnetic susceptibilities were measured under a 5000 G applied magnetic field in the 2−300 K temperature range. The magnetic behavior of **1′** and **2′b** is shown in Figures 6 and 7, respectively, as χ_A and μ_{eff} vs T plots, where χ_A and μ_{eff} are the magnetic susceptibility and effective magnetic moment per copper, respectively. The χ_A vs T curves of **1′** and **2′b** show a maximum at 115 and 100 K, respectively. The effective magnetic moments per copper for **1′** (1.57 μ_B) and **2′b** (1.69 μ_B) at 290 K are smaller than the spin-only value for $S = {}^1/_2$. When the temperature is lowered, the effective magnetic moments decrease gradually, indicating the operation of antiferromagnetic interactions. These magnetic susceptibility data were interpreted quantitatively based on tetranuclear (**1′**) and hexanuclear (**2′b**) cyclic structures, by using the spin Hamiltonian $\mathbf{H} = -2J\Sigma_{i=1,n-1}\mathbf{S}_i\cdot\mathbf{S}_{i+1} - 2J\mathbf{S}_1\cdot\mathbf{S}_n$ where $n = 4$ (**1′**) and 6 (**2′b**), and J is the Heisenberg exchange integral between two adjacent Cu(II) ions. The irreducible tensor operator approach[22,23] was employed to calculate the energy levels of the 4-spin and 6-spin rings, allowing us to take full advantage of the total spin symmetry. Six spin-states with S total spin values ranging from 0 to 2 are obtained for **1′**, while 20 spin states ranging from 0 to 3 are obtained for **2′b**. The CLUMAG program was used to evaluate the matrix elements

(22) Silver, B. L. *Irreducible Tensor Methods*; Academic Press: New York, 1976.
(23) Gatteschi, D.; Pardi, L. *Gazz. Chim. Ital.* **1993**, *123*, 231.

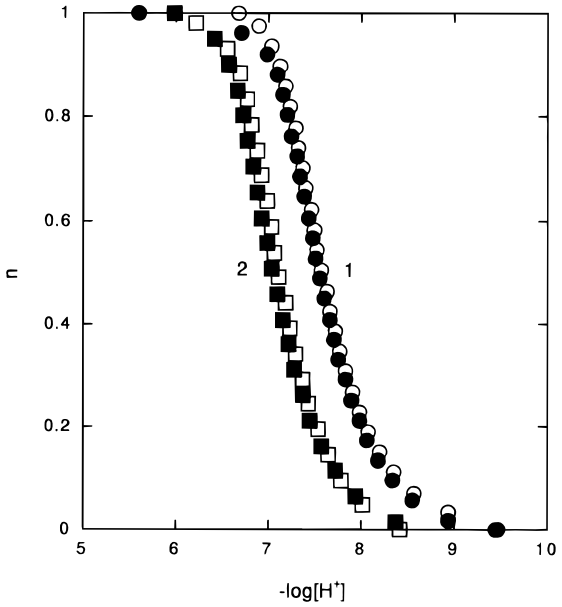

Figure 8. pH-dependent potentiometric titration curves (proton association degree *n* vs pH) for the forward (black) and reverse (white) titrations of **1** (circle) and **2** (square).

(coupled basis set) in the various S blocks which were therefore diagonalized.[23] The magnetic susceptibility per mole was finally calculated with the Van Vleck equation:[24]

$$\chi = [Ng^2\beta^2\Sigma_i S(S+1)(2S+1)\exp(-E_i/kT)]/[3kT\Sigma_i(2S+1)\exp(-E_i/kT)]$$

where N is Avogadro's number, k the Boltzmann constant, and g the Cu(II) Landé factor, and the sum is extended to all the spin states of the ring. The experimental data were fitted to this theoretical equation completed with a paramagnetic term (par) and a constant contribution of 60×10^{-6} cgsu, to take into account the possible presence of Cu(II) monomeric impurities, and temperature independent paramagnetism, respectively. The experimental magnetic data of **1′** and **2′b** are well reproduced in the whole temperature range for the best-fit parameters: $g = 2.03$, $J = -54.7$ cm^{-1}, and par = 0.47% (**1′**); $g = 2.02$, $J = -52.1$ cm^{-1}, and par = 0.54% (**2′b**) (Figures 6 and 7); and $g = 1.98$, $J = -45.7$ cm^{-1}, and par = 3.9% (**2′a**). The calculated J exchange integrals are compatible with those of imidazolate-bridged binuclear Cu(II) complexes in which the imidazolate group bridges the Cu(II) ions at their equatorial sites.[25] The fairly large antiferromagnetic interactions result from a superexchange mechanism in which the unpaired electrons of adjacent Cu(II) ions occupying the orbitals lying in the basal coordination planes interact through the imidazolate bridge.

Potentiometric pH Titration. The reversible interconversions between the Cu(II) monomers and cyclic oligomers have been confirmed by potentiometric pH titration. Figure 8 shows the results of forward and reverse titrations carried out in water at 25 °C (Experimental Section). The degree of proton association n calculated by Bjerrum's method[9,10] decreases from 1 to 0 for the forward titration and increases from 0 to 1 for the reverse titration. The imidazole proton does not dissociate when **1** and **2** are dissolved in pure water (ca 0.25×10^{-3} mol L^{-1} aqueous solution) as indicated by the constant electrode potentials. The forward and reverse titration curves are almost the same, indicating that the deprotonation and protonation are reversible. From these titrations, values of 7.5 and 7.0 were determined for the pK_D dissociation constants of **1** and **2**, respectively. The larger pK_D value for complex **1** compared to **2** may result from the stronger electron donating character of the 2-methyl- compared to the 2-phenylimidazole substituent.

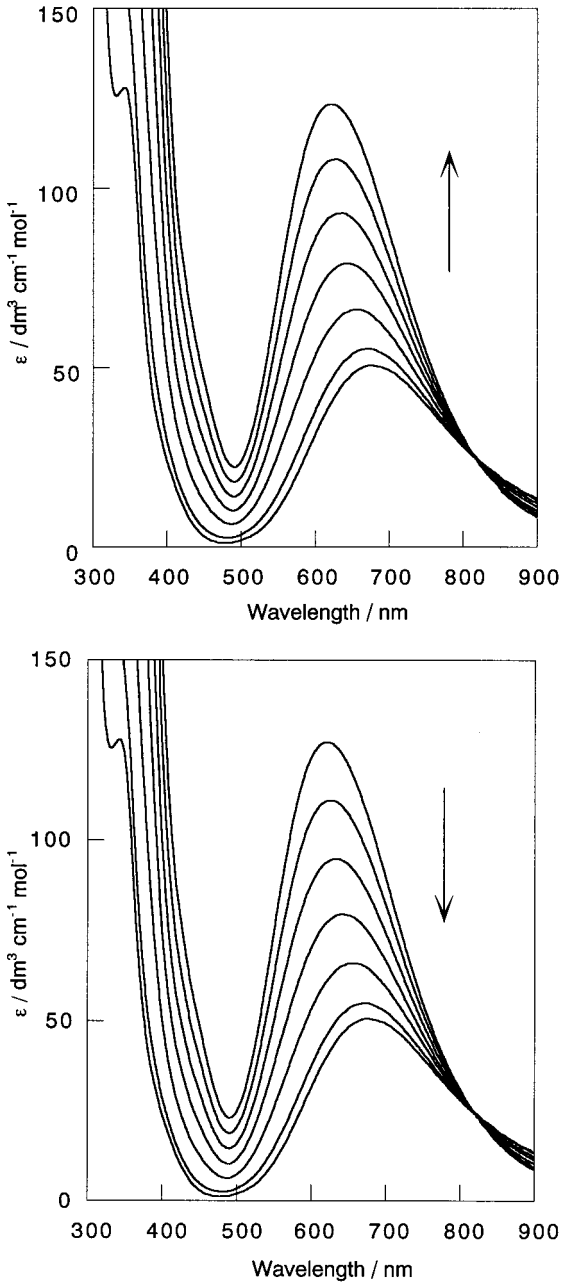

Figure 9. pH-dependent electronic spectra of **1**. An aqueous solution of the protonated complex (0.24 mmol of the complex in 80 mL of water) was prepared. A spectrum was recorded after each 0.4 mL addition of a 0.1 M NaOH solution, until 1 equiv of NaOH was added. Immediately after, electronic spectra were recorded for the reverse titration, following each 0.4 mL addition of a 0.1 M HCl solution to the solution resulting from the forward titration. The spectra were corrected for the volume variation due to the addition of the NaOH and HCl solutions. (top) Forward titration; (bottom) reverse titration.

pH-Dependent Electronic Spectra. The pH-dependent electronic spectra for the **1** → **1′** → **1** and **2** → **2′** → **2** interconversions were measured in aqueous solution (Experimental Section). As a representative result, Figure 9 shows the

(24) Van Vleck, J. H. *The Theory of Electric and Magnetic Susceptibilities*; Oxford University Press: London, 1932.
(25) Matsumoto, N.; Akui, T.; Murakami, H.; Kanesaka, J.; Ohyoshi, A.; Okawa, H. *J. Chem. Soc., Dalton Trans.* **1988**, 1021.

pH-dependent electronic spectra for the **1** → **1′** forward conversion and for the **1′** → **1** reverse conversion. The spectrum of **1** exhibits a broad band at 682 nm (molar extinction coefficient $\epsilon = 48$ M^{-1} cm^{-1}) assignable to a d−d transition. On adding a 0.1 M aqueous NaOH solution, this broad band shifts to lower wavelength and the molar extinction coefficient increases. When the amount of NaOH solution added was equimolar, the generated spectrum had a d−d band maximum at 620 nm ($\epsilon = 127$ M^{-1} cm^{-1}) perfectly consistent with the spectrum of **1′**. This spectral change is characterized by an isosbestic point at 805 nm, typical of an equilibrium between the protonated and deprotonated forms. The spectra for the **1′** → **1** reverse titration exhibit an isosbestic point at the same wavelength and reach the genuine spectrum of **1**, evidencing that the equilibrium is reversible. The pH-dependent electronic spectra for the **1′** → **1** → **1′** interconversion were also investigated confirming the reversibility of the overall process.

The pH-dependent electronic spectra for the **2** → **2′** → **2** interconversion evidenced a behavior similar to that observed for the **1′** ⇌ **1′** couple. The spectrum of **2** exhibits a d−d band at 681 nm ($\epsilon = 59$ M^{-1} cm^{-1}). Upon addition of a 0.1 M NaOH solution, the spectrum changed exhibiting an isosbestic point at 740 nm. When the amount of added NaOH solution was equimolar, the spectrum showed a d−d band maximum at 630 nm ($\epsilon = 105$ M^{-1} cm^{-1}) consistent with the spectrum of **2′**.

Concluding Remarks. The mononuclear Cu(II) complexes **1** and **2** are modular building units able to induce a self-assembly reaction via formation of metal−imidazolate nitrogen coordination bonds between adjacent units, since they potentially assume both donor and acceptor abilities. In addition, the donor ability of the imidazolate nitrogen atom is concealed by the proton at pH lower than the dissociation constant. Because cooperation of the donor and acceptor characters is essential for this self-assembly process, complexes **1** and **2** exist as monomers in acidic medium. In the pH region above the dissociation constant, *i.e.*, in alkaline medium, a self-assembly process due to the cooperation of the donor and acceptor abilities is induced, yielding the imidazolate-bridged oligomers **1′** and **2′**. The size of the self-assembled structures can be tuned through the design of the ligand, as evidenced by the respective tetranuclear and hexanuclear structures of **1′** and **2′**. The reverse disassembling process from oligomeric to mononuclear structures is evidenced by the pH-dependent potentiometric and spectral titrations in aqueous solution. The reversibility is achieved owing to the coordination plasticity of Cu(II) ion. The disassembly process depends on the metal ion, since the Cu(II) complex exhibits a reversible interconversion, whereas the Pd(II) complex did not show a perfect disassembly process.[6a]

Acknowledgment. This work was supported by Monbusho International Scientific Research Program (No. 10044089 "Joint Research") and by a Grant-in-Aid for Scientific Research on Priority Area (No. 10149101 "Metal-Assembled Complexes").

Supporting Information Available: X-ray crystallographic files including the structural data for **1**·H_2O, **1′**·$4H_2O$, **2**, **2′a**·$6H_2O$ and **2′b**, in CIF format, are available free of charge via the Internet at http://pubs.acs.org.

IC981158B